

Imaging depth extension of optical coherence tomography in rabbit eyes using optical clearing agents

Ruiming Kong¹ , Wenjuan Wu¹, Rui Qiu¹, Lei Gao¹, Fengxian Du¹, Ailin Liu², Xuan Cai³  and Cuixia Dai¹

¹College of Sciences, Shanghai Institute of Technology, Shanghai 201418, China; ²State Key Laboratory of Medical Neurobiology, Institutes of Brain Science, Department of Ophthalmology, Zhongshan Hospital, Fudan University, Shanghai 200030, China; ³Department of Ophthalmology, Shanghai Jiao Tong University Affiliated Sixth People's Hospital, Shanghai 200000, China
Corresponding author: Cuixia Dai. Email: sdadai7412@163.com

Impact statement

Imaging depth of optical coherence tomography in ophthalmology is limited by light attenuation in tissues due to inherent optical scattering and absorption. In this study, imaging depth of the anterior and posterior segments of rabbit eyes was extended by using optical clearing agents to reduce multiple scattering. This study may provide a potential method for ophthalmic research, such as accommodation, ocular growth, and biometry of the eye, and for diagnosis of posterior scleritis and intra-orbital tumor, such as orbital cavernous hemangioma, optic nerve glioma, and inflammatory pseudotumor.

Abstract

Optical coherence tomography has become an indispensable diagnostic tool in ophthalmology for imaging the retina and the anterior segment of the eye. However, the imaging depth of optical coherence tomography is limited by light attenuation in tissues due to optical scattering and absorption. In this study of rabbit eye both *ex vivo* and *in vivo*, optical coherence tomography imaging depth of the anterior and posterior segments of the eye was extended by using optical clearing agents to reduce multiple scattering. The sclera, the iris, and the ciliary body were clearly visualized by direct application of glycerol at an incision on the conjunctiva, and the posterior boundary of sclera and even the deeper tissues were detected by submerging the posterior segment of eye in glycerol solution *ex vivo* or by retro-bulbar injection of glycerol *in vivo*. The *ex vivo* rabbit eyes recovered to their original state in 60 s after saline-wash treatment, and normal optical coherence tomography images of the

posterior segment of the sample eyes proved the self-recovery of *in vivo* performance. Signal intensities of optical coherence tomography images obtained before and after glycerol treatment were compared to analysis of the effect of optical clearing. To the best of our knowledge, this is the first study for imaging depth extension of optical coherence tomography in both the anterior and posterior segments of eye by using optical clearing agents.

Keywords: Optical coherence tomography, tissue optical clearing technology, optical clearing agents, rabbit eye, glycerol, retro-bulbar injection

Experimental Biology and Medicine 2020; 245: 1629–1636. DOI: 10.1177/1535370220949834

Introduction

Optical coherence tomography (OCT) is a non-invasive imaging technique, which can perform high-resolution cross-sectional imaging of biomedical tissues.¹ OCT is suitable for diagnostic applications in ophthalmology because of the ease of optical access to the anterior and posterior segments of the eye. In recent years, it has become a clinical standard for diagnosing eye disease and monitoring treatment.² However, light attenuation in tissues, which is caused by optical scattering and absorption of biological substances, limits the penetration of light and thus the depth of OCT imaging.^{3,4}

Several research groups have used OCT to observe the dynamic process of eye accommodation. The changes of crystalline lens and ciliary muscle during accommodation were clearly imaged. However, the eye accommodation theory is still unconfirmed since the suspensory ligament cannot be imaged due to light attenuation. Orbit diseases, such as intra-orbital tumor and orbital inflammation, result in severe damage to vision and always distress the patient. Because of the specific deep location, B-mode ultrasound and MRI have been commonly used for the diagnosis of orbit disease.^{5,6} However, although B-mode ultrasound and MRI provide images of tumor boundaries at low resolution,

they cannot provide information about the mechanism of the tumor growth, especially the neovascularization features. OCT has been used to image the structure and function of the fundus, and even the vascular of choroidal tumors,⁷ but due to the limitation of imaging depth, there have been no reports of OCT imaging of intra-orbit tumor or orbital inflammation.

For deeper structure imaging, some techniques like the enhanced depth imaging OCT (EDI-OCT) and averaging multi-images at the same scan position are used.⁸ OCT with an electrically tunable lens (ETL) can enhance the signal-to-noise ratio (SNR) of deeper tissues by dynamically controlling the focusing of the probe light beam.⁹ However, EDI-OCT, multi-images averaging, and ETL technology do not improve light penetration, so the imaging depth of OCT is not improved. Reduction of the optical scattering and absorption in tissues is highly desired. Since melanin plays a dominant role for light absorption in the iris and choroid,¹⁰ techniques have been proposed to bleach melanin by potassium permanganate (KMnO₄) and hydrogen peroxide (H₂O₂).¹¹ However, since bleaching using KMnO₄ and H₂O₂ is an irreversible and harmful process, it is not a feasible technique for *in vivo* imaging.

Considering optical scattering, light sources with longer wavelength have been generally used due to the smaller scattering coefficient; 1.3 μm wavelength centered light sources are used for the anterior segment of eye imaging and 1.0 μm wavelength centered light sources are used for the posterior segment of eye imaging. For optical scattering reduction to enhance light depth penetration, a tissue optical clearing (TOC) technique was proposed to reduce light scattering by using optical clearing agents (OCAs), which decrease the difference of refractive index between tissues.^{6,12} In this technique, glycerol and glycerol-water solution, glucose, propanediol, polyethylene glycerol, polypropylene glycerol, oleic acid, and DMSO are typically used.¹³ Thick tissues, even heart, liver, and bones of mouse become transparent after optical clearing treatment.¹⁴ Eye tissues, such as sclera and cornea of rabbit eyes, can be partly optically cleared by metronidazole, dexamethasone, ciprofloxacin, mannitol, or glucose solution.^{15,16} However, most OCAs change the sample volume

and decrease microvascular density.¹⁷ This is the reason why it is hard to use them in tissues *in vivo*. A clinically approved solution for *in vivo* tissue is glycerol. Glycerol was used as OCA by dermal injection in rat dorsal skin *in vivo*¹⁸ and on mouse cranial nerve *in vivo* through a skull optical clearing window.¹⁹ Safety of the glycerol treatment and self-recovery of tissues were also demonstrated.²⁰ To the best of our knowledge, the only optical clearing study in ophthalmology *in vivo* is the recently reported work on the anterior segment of rabbit eye by glycerol treatment through an incision on the conjunctiva, in which transparency and later on recovery of the sclera were proved.²¹ However, for the eye which is a special organ, they did not try the TOC study on the internal segment.

Here, we present our work on imaging depth extension for OCT imaging of rabbit eyes *ex vivo* and *in vivo*. Both the anterior and posterior segments of the rabbit eyes were optically cleared by using TOC. Optical clearing of the anterior segment was performed by applying glycerol solution through an incision on the conjunctiva. For optical clearing of the posterior segment, half of the excised eye was submerged in glycerol solution. For *in vivo* experiments, the rabbit eye was treated by retro-bulbar injection of glycerol to the intra-orbital area of the eye. Signal intensities of OCT images obtained with or without applying OCA treatment were compared to evaluate the optical clearing effect. Self-recovery of the eyes was also proved.

Materials and methods

All animal procedures were approved by Shanghai Jiao Tong University Affiliated Sixth People's Hospital.

Experimental system

A customized spectral domain OCT (SD-OCT) system centered at 840 nm was built to image both the anterior and posterior segments of the eye and to test the optical clearing effect. A schematic of the system is shown in Figure 1. The light source was a super luminescent diode (SLD, Inphenix Inc., USA) with a full width at half maximum (FWHM) bandwidth of 53 nm. The light from the SLD was split into the reference and the sample arms of a Michelson

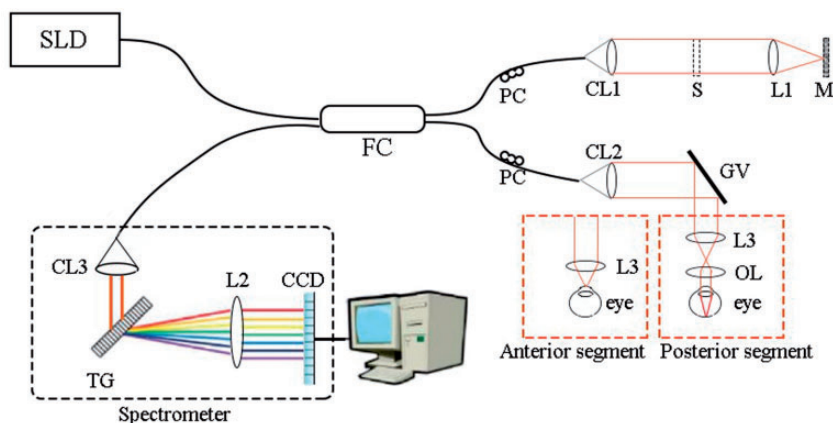


Figure 1. Schematic diagram of SD-OCT system. FC: fiber coupler; CL: collimating lens; S: slit; L: lens; GV: galvo; M: mirror; TG: transmission grating; PC: polarization controller; OL: ocular lens. Dotted box is the probes for anterior segment and retina imaging respectively. (A color version of this figure is available in the online journal.)

interferometer. In the sample arm, the illuminating light propagated to the eye through a collimator, a dual-axis galvo system (GVS002; Thorlabs Inc., USA), and an objective lens ($f = 50$ mm) for OCT imaging of the anterior segment of the eye. The light was further collimated by an ocular lens (60D, Veatch Ophthalmic Instruments, USA) and finally focused on the retina by the anterior segments of the eye for the posterior segment imaging. In the reference arm, the light was propagated through a collimator, a lens, and a mirror. The backreflected and backscattered light from the reference and the sample arms generated spectral interference signals to be detected by a spectrometer, which consists of a 1800 line/mm grating, a multi-elements imaging lens ($f = 100$ mm), and a line scan CCD camera (Aviivaiva-SM2-CL-2014, 2048 pixels with $14 \mu\text{m}$ pixel size, Teledyne e2v Ltd., England). The linear CCD camera was operated at a rate of 20 kHz with an integration time of $36 \mu\text{s}$. Image acquisition boards (NI IMAQ PCI 1428, USA) acquired the images captured by the camera and transferred them to a computer for signal processing and image display. Imaging depth of the OCT system was 3.6 mm. The axial resolution of the system was $6.2 \mu\text{m}$. The lateral resolution of the system for the anterior segment imaging was measured as $9.6 \mu\text{m}$, and that for the posterior segment imaging was measured as $14.2 \mu\text{m}$. The light power on the eye sample was 1.25 mW which was well below the safe cut-off value according to the American National Standard Institute (ANSI) Z136.1.

Samples and materials

In this study, rabbits (SPF Dutch Belted, female, eight-weeks, 2 kg) and rabbit eye samples were provided by Shanghai Jia Gan Biotechnology Co., Ltd (Shanghai, China). Three rabbit eye samples were used to observe the optical clearing effect of the anterior and posterior segments. The redundant tissues such as muscles on the *ex vivo* eye sample were removed for quick optical clearing. Three rabbits were used in the experiments *in vivo*. Pentobarbital sodium solution (30 mg/kg intravenous) was used for anesthesia. For both the *ex vivo* and *in vivo* procedures, 75% anhydrous glycerol mixed with salt solution was used as OCA.²²

In the *ex vivo* experiments, a 0.3 cm wide incision was made on the conjunctiva to allow adequate contact of glycerol for the anterior segment.²³ Half of the eye was immersed in glycerol solution in a culture dish container for optical clearing of the posterior segment. A piece of paper tissue was placed between the eye and the container to ensure the full contact with glycerol. The design of the eyeball-paper tissue-container simulated the eye in orbit, which can provide an important reference for *in vivo* study. In the *in vivo* experiments, a 0.3 cm incision was also made in the conjunctiva, and glycerol solution was added to the sclera for optical clearing of the anterior segment. Optical clearing of the posterior segment was performed by retro-bulbar injection, which is a common surgical procedure in ophthalmology and widely used in rabbit experiments.²⁴ In the experiment, a long needle (KOL, $5 \times 0.5 \times 38$ twl) suitable for retro-bulbar

performance was used, and glycerol solution was injected into the posterior sclera and posterior interstitial space to make sure that the sclera and the posterior interstitial tissue can be treated simultaneously. The details of the retro-bulbar injection were as follows: when the rabbit was completely anesthetized and the periorbital area was sterilized with povidone-iodine, the rabbit eye was opened by a speculum (MR-0103-1, Xiehe medical instrument, China). The needle was at first advanced tangentially to the globe and parallel to the orbital floor, and then was directed superiorly and into the intra-orbital area. Finally, the needle was inserted 7 mm deep below the lacrimal gland and the glycerol was injected. After injection, the needle was slowly pulled out and the eye was gently pressed for about 10 min to help the spread of glycerol in the posterior segment.

In the experiment, the *ex vivo* eye samples and the anterior segment of *in vivo* eyes were treated by drops of saline solution at eye surface to promote recovery. Short-term and long-term observation of the posterior segment of *in vivo* eyes was also conducted to prove self-recovery of the eye.

Results

Ex vivo optical clearing performance

Photos. Photos of the eye sample are shown in Figure 2. The dynamic processes of optical clearing of the anterior and the posterior segments can be seen from the appearance. Comparing the images in the area marked by a dotted box in Figure 2(a) and (b), the anterior segment is transparent enough to see through the sclera to the aqueous humor at 25 min after being applied drops of glycerol solution. For the posterior segment, optical clearing was performed by submerging the posterior segment of the eye in glycerol solution. As we can see from Figure 2(c) to (e), the eye is still opaque after being immersed in glycerol solution for 10 min. The optical clearing effect can be observed after 10 min as shown in Figure 2(f) and (g). The posterior segment becomes totally transparent after 25 min, and vessels on the retina can be visualized, as shown in Figure 2(h).

The recovery ability of the *ex vivo* eyes was proved by washing with saline solution. The dynamic process of recovery was monitored for 60 s. In the first 20 s as shown in Figure 3(a) to (c), the sclera slowly became opaque. In the next 20 s, most parts of the sclera are opaque as shown in Figure 3(d) and (e). Finally, the whole posterior segment recovers to its original state and is totally opaque in the last 20 s as shown in Figure 3(f).

OCT images. Figure 4 shows OCT images of the anterior and posterior segments of the rabbit eyes *ex vivo*, the depth of which is significantly extended after optical clearing treatment. Before glycerol treatment, the boundary of the sclera and the ciliary body cannot be clearly identified and the suspensory ligament cannot be detected due to light attenuation by the sclera, as shown in Figure 4(a). After 25 min of treatment with glycerol, as shown in Figure 4 (b), the ciliary muscle is clearly imaged: the boundary of

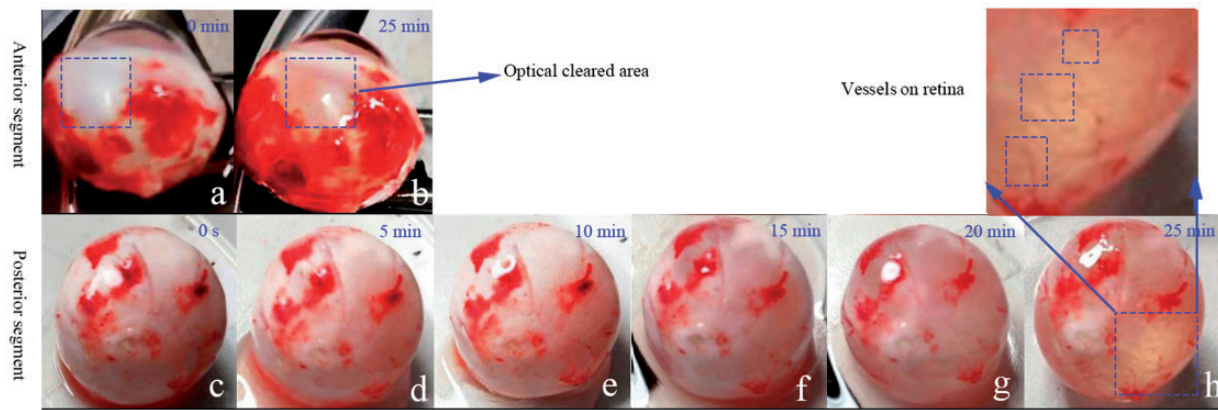


Figure 2. Dynamic process of optical clearing of *ex vivo* rabbit eyes. Anterior segment: (a) without glycerol treatment. (b) 25 min after glycerol treatment. Posterior segment: (c) without glycerol treatment. (d)–(h) 5, 10, 15, 20, 25 min after glycerol treatment. The dotted box indicates the optical clearing area. (A color version of this figure is available in the online journal.)

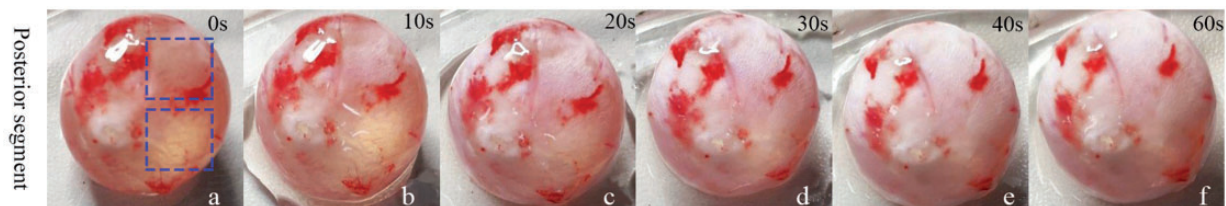


Figure 3. Recovery of *ex vivo* eyes. (a) Without treatment of saline. (b)–(f) 10, 20, 30, 40, 60 s after treatment of saline. The dotted box indicates the optical recovering area. (A color version of this figure is available in the online journal.)

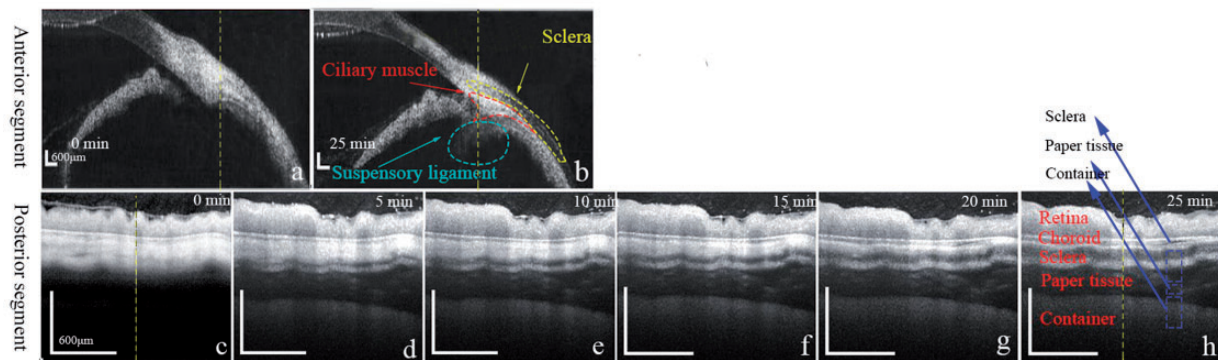


Figure 4. *Ex vivo* OCT images of rabbit eyes. Anterior segment: (a)–(b) 0, 25 min after glycerol treatment; Posterior segment: (c) without glycerol treatment. (d)–(h) 5, 10, 15, 20, 25 min after glycerol treatment. The dotted box indicates area of intensity enhancement. Yellow line: A-Line pixels for quantitative comparison. (A color version of this figure is available in the online journal.)

ciliary muscle and even the deeper tissue can be imaged (marked in the dotted region).

The time course of optical clearing on the posterior segment is given in Figure 4(c) to (h). Without treatment with glycerol as shown in Figure 4(c), the boundary of the sclera cannot be differentiated. The paper tissue and the container are hard to be detected due to light attenuation. After 5 min of immersing in glycerol solution, as shown in Figure 4(d), the boundary between the posterior choroid, the paper tissue, and the container begins to be detected. For the next 20 min, OCT image contrast is further increased. The paper tissue and the container are clearly imaged, as shown in the dotted box in Figure 4(h). Quantitative analyses of

imaging depth extension of OCT for both the anterior and posterior segments of the rabbit eye *ex vivo* were performed by comparison of A-line pixel intensities of OCT images (marked by yellow dotted lines in Figure 4) obtained before and after glycerol treatment, as shown in Figure 5. Signal intensities, averaged along the A-Line pixels at regions of the sclera, the ciliary muscle and the suspensory ligament in the anterior segment and the sclera, the paper tissue, and the container in the posterior segment were analyzed to show the optical clearing effect. As seen from the green-box regions in Figure 5(a), signal intensity of the sclera is decreased after glycerol treatment, and those of the ciliary muscle and the suspensory ligament are

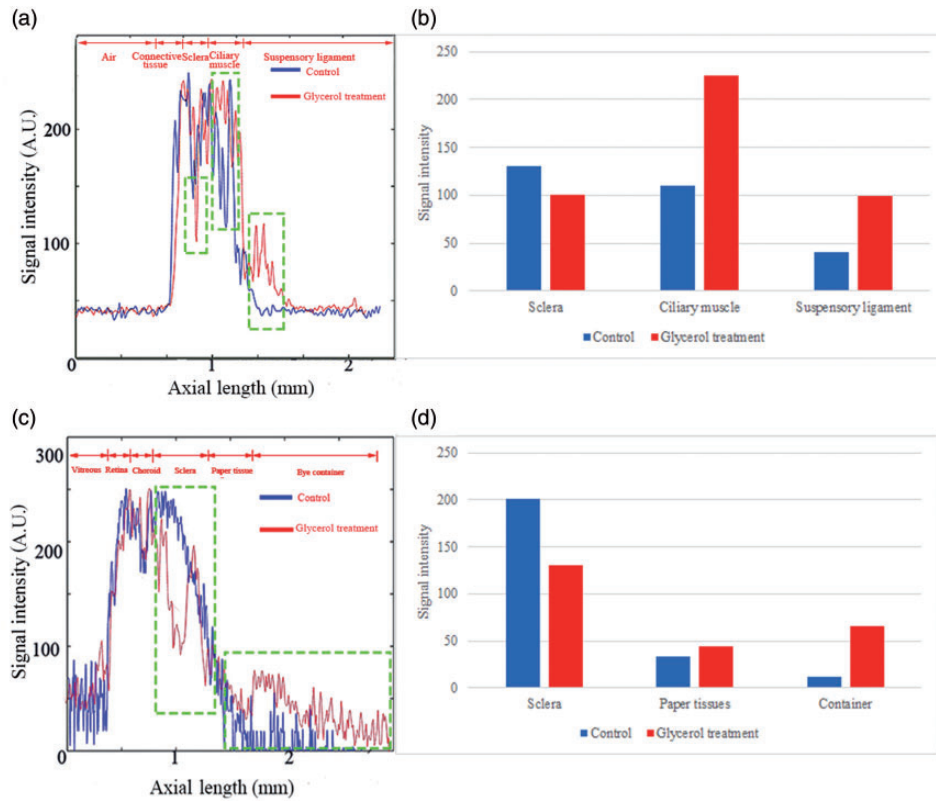


Figure 5. Quantitative analyses of imaging depth extension of *ex vivo* OCT. (a) A-line pixel intensities of the anterior segment along the yellow lines in Figure 4(a) and (b); (b) signal intensities averaged at each region in the anterior segment; (c) A-line pixel intensities of the posterior segment along the yellow lines in Figure 4(c) (h); (d) signal intensities averaged at regions in the posterior segment. (A color version of this figure is available in the online journal.)

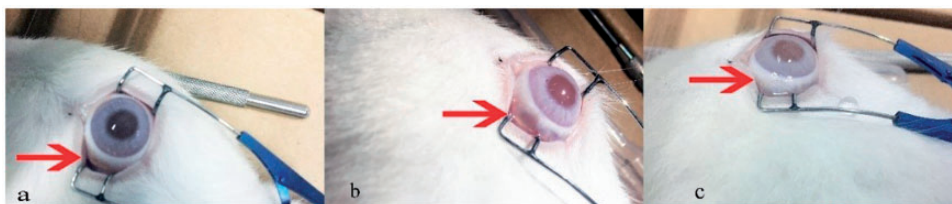


Figure 6. Photos of rabbit eye. (a) Before glycerol treatment. (b) 25 min after glycerol treatment. (c) 60 s after saline wash. The red arrow indicates the position of the incision. (A color version of this figure is available in the online journal.)

increased. Light propagated into the deep tissues because optical scattering decreases in the sclera, and thus both the ciliary muscle and the suspensory ligament are well imaged, which is further demonstrated by signal intensities averaged along the A-Line at these regions as shown in Figure 5(b). A-line pixel intensities of tissues in the posterior segment (marked by yellow dotted lines in Figure 4(c) and (h)) are shown in Figure 5(c). From regions marked by the green box, we can see that signal intensity of the sclera is obviously decreased, and those of the paper tissue and container are increased. Signal intensities averaged at the regions of the sclera, the paper tissue, and the container, as shown in Figure 5(d), also demonstrate the imaging depth extension performance. After optical clearing treatment, the signal intensity of the sclera is doubly decreased and those of paper tissue and the container are increased. We can see that optical clearing and imaging depth extension of OCT are successfully performed in the experiments.

In vivo optical clearing performance

Photos. The optical clearing effect on the anterior segment of the rabbit eye can be seen from the photos. After the rabbit was anesthetized by Pentobarbital Sodium solution, an incision was made on the conjunctiva with a micro scalpel (Mingren, MR-K114, China), as shown in Figure 6(a). The eye becomes transparent in 25 min after glycerol treatment, as shown in Figure 6(b). The recovery process was also performed by saline wash as in the *ex vivo* experiment, and the sclera became completely opaque after 60 s, as shown in Figure 6(c).

OCT images. Figure 7 shows the OCT images of the anterior and posterior segments of rabbit eyes *in vivo*. Figure 7 (a) and (b) demonstrates the B-scan OCT images of the anterior segment of the rabbit eye before and after glycerol treatment, respectively. Twenty-five minutes after glycerol treatment, the sclera and the ciliary body are clearly imaged

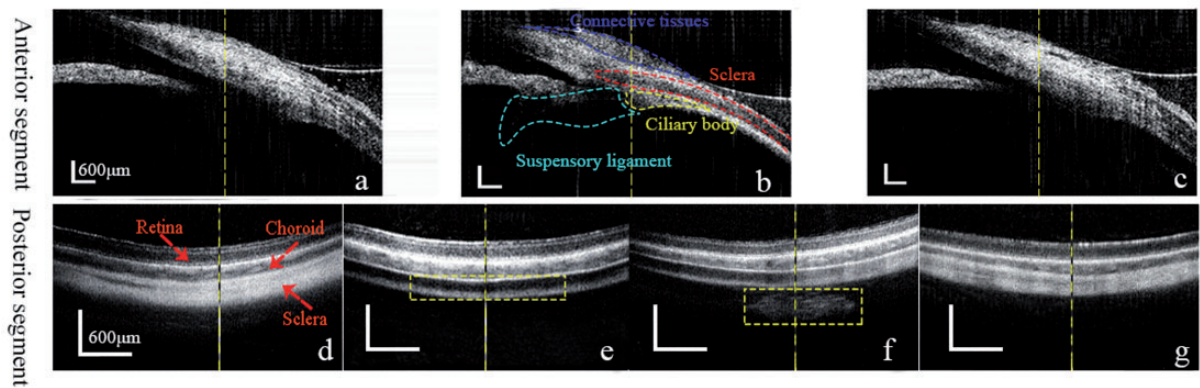


Figure 7. *In vivo* OCT images of rabbit eyes. Anterior segment: (a) before glycerol treatment. (b) 25 min after glycerol treatment. (c) 60 s after saline solution treatment. Posterior segment: (d) before glycerol treatment. (e) 25 min after glycerol treatment. (f) 25 min after glycerol treatment. (g) Three days after glycerol treatment. Imaging depth extension of OCT is indicated by the dotted lines in each image. Yellow line: A-Line pixels for quantitative comparison. (A color version of this figure is available in the online journal.)

and their boundaries are obviously differentiated. The suspensory ligament was also imaged; 60 s after just saline dropping with a dropper on the eye surface, the OCT image recovers to its original state, as shown in Figure 7(c).

Imaging depth extension of OCT of the posterior segment is shown in Figure 7(d) to (g). Due to high light scattering in tissues, the posterior boundary of the sclera cannot be clearly imaged, as shown in Figure 7(d). Twenty-five minutes after glycerol treatment by retro-bulbar injection, the sclera and the boundary between posterior the choroid and the sclera are clearly imaged, as shown in Figure 7(e). From Figure 7(f), we can see that deep tissues in the intra-orbital area can even be detected. Three days after the optical clearing performance experiment, an OCT image of healthy fundus was obtained from the same eye as shown in Figure 7(g) which proves the self-recovery of the rabbit eye and the safety of the *in vivo* procedure.

Quantitative analyses were performed as those in the *ex vivo* experiments, and the results also prove the imaging depth extension of *in vivo* OCT. The A-line pixel signal intensity and the signal intensities averaged along the A-line pixels of the anterior segment (along the dotted lines in Figure 7(a) to (c)) are given in Figure 8(a) and (b), respectively. Since connective tissues will prevent the diffusion of glycerol in live tissues, the optical clearing effect in the anterior segment in *in vivo* studies is not as remarkable as that in *ex vivo* studies, as shown in Figure 8(a) and (b). After the sclera is optically cleared, signal intensities of the ciliary and the suspensory ligament are increased.

Signal intensities of the posterior segment (along the dotted lines in Figure 7(d) to (g)) are given in Figure 8(c) and (d). After glycerol treatment by retro-bulbar injection, signal intensity of the sclera is obviously decreased, as shown by the red lines in Figure 8(c), and the signal intensities of deeper tissues are increased as indicated by the green lines. Signal intensity of the sclera is decreased to 30% and that of intra-orbital tissues is doubly increased, as shown in Figure 8(d). Comparing signal intensities obtained before glycerol treatment and after saline treatment for the anterior segment (as shown in Figure 8(a) and (b)), and those obtained before glycerol treatment

and three days after glycerol treatment for the posterior segment (as shown in Figure 8(c) and (d)), we can see that the anterior and posterior segments will recover by saline wash or by the self-metabolism.

Discussion

In this paper, we presented our work on depth extension of OCT imaging of the anterior segment and posterior segment of the rabbit eye using the TOC technique. Satisfactory results were demonstrated in both *ex vivo* and *in vivo* studies of the anterior segment: clear images of deep tissue such as ciliary body were obtained and the eye quickly recovered just by saline wash intervention. Since the crucial issue for the *in vivo* performance is eye safety, we performed both short-term and long-term monitoring of the eye sample. The conjunctiva of the eye had slight chemosis at 2 h after the retro-bulbar injection. The morphological change slowly disappeared and the eye seemed to be normal after 5 h. None of the rabbits used in the experiments displayed adverse effects such as weight loss, distress, skin lesions due to inflammation, granulomas, infection, alopecia, or graft rejection. When the rabbit awoke after injections, no abnormalities in eye movements were observed. Three days later, we covered the unused eye with a piece of black cloth and placed the feed 1 m away from the rabbit to test its eyesight. The rabbit went directly to the feed, indicating the atraumatic self-recovery of the eye. In the dissection of orbital content after animal death, no inflammation or graft migration was observed.

We would like to mention that the results we presented in this paper were obtained just at a single B-scan using light source centered at 840 nm. By combination of techniques of EDI-OCT, multi-images-averaging and longer wavelength (centered at 1.0 μm), the OCT images will demonstrate more deep tissues with much higher contrast. As seen in Figure 7(f), the deep tissues in the intra-orbital area can even be detected in just one OCT B-scan with 840 nm wavelength. By combination of techniques above, posterior sclera and more orbit tissues may be clearly shown which can provide evidence of posterior scleritis and orbit diseases with high resolution.

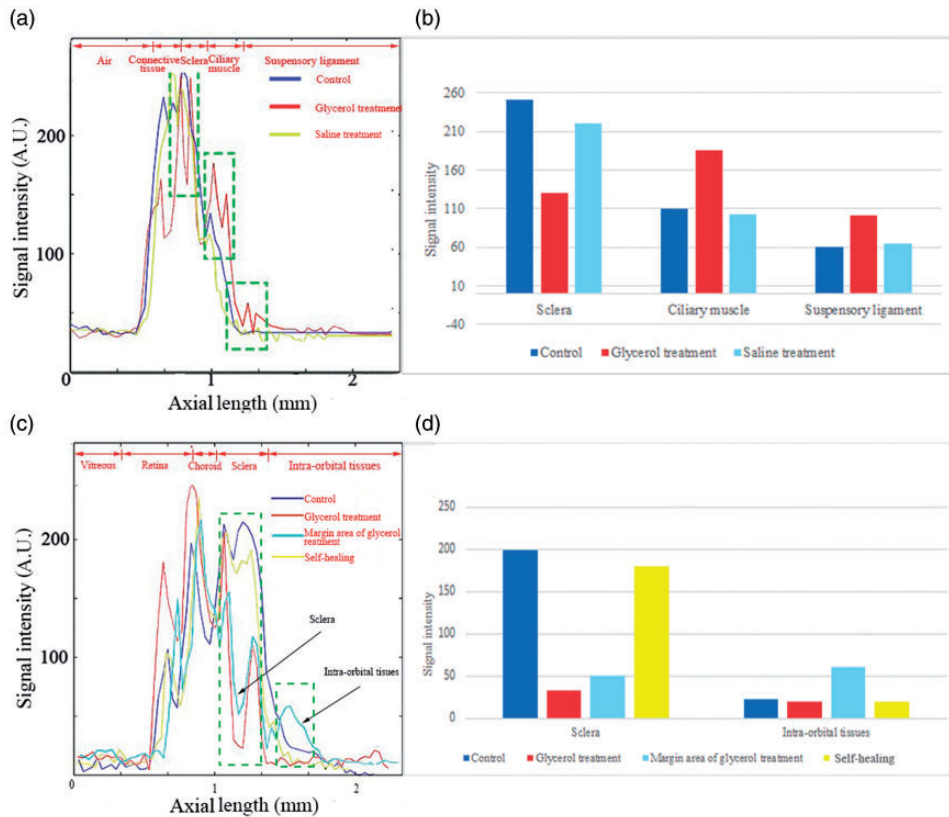


Figure 8. Quantitative analyses of the imaging depth extension of *in vivo* OCT. (a) A-line pixel intensities of the anterior segment along the yellow lines in Figure 7(a) to (c); (b) signal intensities averaged at each region in the anterior segment; (c) A-line pixel intensities of the posterior segment along the yellow lines in Figure 7(d) to (g); (d) signal intensities averaged at each region in the posterior segment. (A color version of this figure is available in the online journal.)

We admit that only light attenuation caused by optical scattering was considered in our study. For other samples like human eyes, light absorption of biological substances in eyes such as melanin is another important factor of light attenuation. However, light absorption of biological substances in the eyes is unavoidable, and this remains an issue to overcome for deep depth imaging. Melanin, a pigment derived from tyrosine via a multistep reaction that includes oxidation and polymerization, is the main absorbent of light in the tissue. Research has shown that an effective melanin removing method in eyes is melanin bleaching by some strongly oxidizing substances, like potassium permanganate (KMnO_4) with oxalic acid and 10% hydrogen peroxide (H_2O_2).¹⁰ Since KMnO_4 /oxalic acid demonstrates poor depigmentation with extensive tissue damage, the optimal bleaching is achieved using warm 10% H_2O_2 diluted in PBS at 65°C for about 120 min. However, these methods will take a long time. High temperature will destroy the physiological structure of tissue, and the melanin bleaching process is irreversible. They are therefore impracticable for *in vivo* performance. In our study, imaging depth extension of OCT imaging of eyes is demonstrated through reduction of the light scattering by highly effective OCAs. Methods of rapid reduction of light absorption with appropriate eye processing are recommended in the further study.

In summary, we proposed a useful method to extend the imaging depth of OCT for the anterior and posterior segments of rabbit eyes by means of OCAs. The technique may

help to support the eye accommodation theory by providing deeper cross-sectional structure images in the anterior segment of eyes. It could also help to investigate the neovascularization of intra-orbital tumors in the growing process, and the pathology of orbital inflammation. Moreover, as the safety has been proved, drug therapy of orbit disease such as orbital cellulitis, ocular fasciitis, inflammatory pseudotumor, and angiocavernoma could also be investigated.

Authors' contributions: All authors participated in the design, interpretation of the studies and analysis of the data and review of the manuscript. RMK conducted the experiments and contributed to data analysis and manuscript preparation; WJW, RQ, LG, FXD contributed to experiments and data analysis; ALL supplied critical reagents; XC contributed to the surgery; CXD conceived the project, supervised the study, contributed to data analysis and manuscript preparation.

ACKNOWLEDGMENTS

The authors would like to thank professor Dan Zhu for guidance of TOC technology and thank Dr. Xiangning Wang and Dr. Xinmin Lu for the clinic surgical operation of retro-bulbar injection, thank Dr. Shiqing Zhao for the help of rabbit anesthetized.

DECLARATION OF CONFLICTING INTERESTS


The author(s) declared no potential conflicts of interest with respect to the research, authorship, and/or publication of this article

FUNDING

The author(s) disclosed receipt of the following financial support for the research, authorship, and/or publication of this article: This work was supported by the Natural National Science Foundation of China (61675134, 61307015, 81827807), Science and technology innovation project of Shanghai Science and Technology Commission (19441905800), Project of State Key Laboratory of Ophthalmology, Optometry and Visual Science, Wenzhou Medical University(K181002).

ORCID iDs

Ruiming Kong  <https://orcid.org/0000-0002-6293-3389>

Xuan Cai  <https://orcid.org/0000-0003-4012-2726>

REFERENCES

- Huang D, Swanson E, Lin C, Schuman J, Stinson W, Chang W, Hee M, Flotte T, Gregory K, Puliafito C, Fujimoto J. Optical coherence tomography. *Science* 1991;**254**:1178–81
- Grulkowski I, Liu J, Potsaid B, Jayaraman V, Chen D, Jiang J, Cable A, Duker J, Fujimoto J. Anterior segment and full eye imaging using ultrahigh speed swept source OCT with vertical-cavity surface emitting lasers. *Biomed Opt Express* 2012;**3**:2733–51
- Tuchin V. Tissue optics and photonics: light-tissue interaction. *J Biomed Photon Eng* 2015;**1**:98–134.
- Susaki U. Whole-body and whole-organ clearing and imaging techniques with single-cell resolution: toward organism-level systems biology in mammals. *Cell Chem Biol* 2016;**23**:137–57
- Dallaudiere B, Benayoun Y, Boncoeur-Martel MP, Robert PY, Adenis JP, Maubon A. Aspect des hémangiomes caverneux intraorbitaires. *J Radiol* 2009;**90**:1039–45
- Lekovic GP, Schwartz MR, Hanna G, Go J. Intra-Orbital meningioma causing loss of vision in neurofibromatosis type 2: case series and management considerations. *Front Surg* 2018;**5**:60
- Cennamo G, Romano MR, Breve MA, Velotti N, Reibaldi M, Crecchio G, Cennamo G. Evaluation of choroidal tumors with optical coherence tomography: enhanced depth imaging and OCT-angiography features. *Eye* 2017;**1**–10
- Spaide R, Koizumi H, Pozonn M. Enhanced depth imaging Spectral-Domain optical coherence tomography. *Am. J. Ophthalmol* 2008;**146**:496–500
- Ireneusz G, Silestre M, Lukasz C, Franciszek S, Karol K, Pablo A. Swept source optical coherence tomography and tunable lens technology for comprehensive imaging and biometry of the whole eye. *Optica* 2017;**5**:52–9
- Tainaka K, Kubota S, Suyama T, Susaki E, Perrin D, Tadenuma M, Ukai H, Ueda H. Whole-Body imaging with single-cell resolution by tissue decolorization. *Cell* 2014;**159**:911–24
- Manicam C, Pitz S, Brochhausen C, Grus F, Pfeiffer N, Gericke A. Effective melanin depigmentation of human and murine ocular tissues: an improved method for paraffin and frozen sections. *PLoS One* 2014;**9**: e102512
- Tuchin V, Maksimova I, Zimnyakov D, Kon I, Mavlutov A, and, Mishin A. Luminescence monitoring of temporal changes and efficiency of tissue optical clearing by NIR-excited upconversion particles. *BioNanoScience* 1996;**6**:169–75
- Zhu D, Larin K, Luo Q, Tuchin V. In vivo skin optical clearing by glycerol solutions: mechanism. *J Biophoton* 2010;**3**:44–52
- Jing D, Zhang S, Luo W, Gao X, Men Y, Ma C, Liu X, Yi Y, Bugde A, Zhou B, Zhao Z, Yuan Q, Feng J, Gao L, Ge W, Zhao H. Tissue clearing of both hard and soft tissue organs with the PEGASOS method. *Cell Res* 2018;**28**:803–18
- Ghosn MG, Tuchin VV, Larin KV. Nondestructive quantification of anolyte diffusion in cornea and sclera using optical coherence tomography. *Invest Ophthalm Vis Sci* 2007;**48**:2727–33
- Ghosn MG, Carbajal EF, Befrui NA. Differential permeability rate and percent clearing of glucose in different regions in rabbit sclera. *J Biomed Opt* 2008;**13**:021110
- Loren M, Crouzet C, Bahani A, Vasilevko V, Choi B. Optical clearing potential of immersion-based agents applied to thick mouse brain sections. *PLoS One* 2019;**14**:e0216064
- Shi R, Guo L, Zhang C, Feng W, Li P, Ding Z, Zhu D. A useful way to develop effective in vivo skin optical clearing agents. *J Biophotonics* 2017;**10**:887–95
- Zhao Y, Yu T, Zhang C, Li Z, Luo Q, Xu T, Zhu D. Skull optical clearing window for in vivo imaging of the mouse cortex at synaptic resolution. *LIGHT-SCI. Light Sci Appl* 2018;**7**:17153
- Zhu D, Zhang J, Cui H, Mao Z, Li P, Luo Q. Short-term and long-term effects of optical clearing agents on blood vessels in chick chorioallantoic membrane. *J Biomed Opt* 2008;**13**:021106
- Zaman R, Rajaram N, Nichols B, Rylander III, Wang T, Tunnell J, Welch A. Changes in morphology and optical properties of sclera and choroidal layers due to hyperosmotic agent. *J Biomed Opt* 2011;**16**:077008
- Son T, Jung B. Cross-evaluation of optimal glycerol concentration to enhance optical tissue clearing efficacy. *Skin Res Technol* 2014;**21**:327–32
- Feng Y, Simpson T. Corneal, limbal, and conjunctival epithelial thickness from optical coherence tomography. *Optom Vision Sci* 2008;**85**:880–3
- Cakir B, Aygit A, Okten O, Yalcin O. Retro-Orbital intraconal fat injection: an experimental study in rabbits. *J Oral Maxillofac Surg* 2012;**70**:242–50

(Received January 3, 2020, Accepted July 23, 2020)